Inorganic Chemistry

Article

pubs.acs.org/IC

Optical Response of a Cyclometalated Iridium(III) Hydrazino Complex to Carbon Dioxide: Generation of a Strongly Luminescent Iridium(III) Carbazate

Kyle R. Schwartz and Kent R. Mann*

Department of Chemistry, University of Minnesota, Minneapolis, Minnesota 55455, United States

Supporting Information

ABSTRACT: A system pairing the luminescent core of $[Ir(ppy)_2L_2]^+$ (ppy = 2-phenylpyridine) with simple hydrazino ancillary ligands (L = N_2H_4) has been prepared for the direct optical detection of carbon dioxide (CO_2). Silver-assisted and silver-free techniques were used for the successful introduction of N_2H_4 into the $[Ir(ppy)_2Cl]_2$ coordination sphere at room temperature to give the corresponding biscyclometalated iridium(III) hydrazino species as either a $CF_3SO_3^-$ (OTf^-, **2a**) or Cl^- (**2b**) salt. The silver-free route was accomplished by the direct replacement of the ligated Cl^- using a slight excess of hydrazine. The luminescence profile of the cationic iridium(III) hydrazino complex **2a** (λ_{max} = 501 nm) undergoes a red shift (λ_{max} = 524 nm), accompanied by a change in the peak shape during exposure to CO_2 in solution. The spectral changes observed are attributed to the formation of the corresponding neutral carbazate species $Ir(ppy)_2(H_2NNHCOO)$ (**3**) and are not consistent with protonation of the ligated hydrazine. Conversion of the hydrazino species to the carbazate species is solvent-dependent and irreversible. The hydrazino and carbazate species have been structurally characterized by single-crystal X-ray diffraction; both compounds exhibit long-lived and intense room temperature luminescence in solution with τ = 1.56 and 1.80 μs and ϕ_{em} = 0.42 and 0.45, respectively.

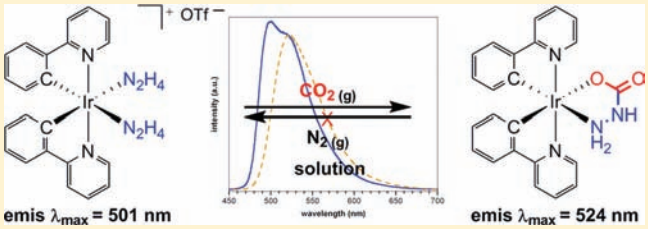

INTRODUCTION

The interaction of small molecules with transition-metal complexes is a topic of wide interest and diversity and holds importance for many facets of scientific research. The use of O_2 in photodynamic therapy,[1] NO in biological messaging,[2] N_2 as an industrial feedstock,[3] and H_2O for the production of H_2 fuel[4] represent a few of the most notable examples. Increased attention toward the level of greenhouse gases such as carbon dioxide (CO_2) in the atmosphere has revived interest in the small molecule as a target of activation,[5] sequestration,[6] and, of particular appeal to our research group, optical detection using either colorimetric[7] or luminescent[8] sensing. The relatively inert nature of CO_2 has proven these to be difficult objectives. Most optical detection schemes previously developed for CO_2 use indirect detection methods that rely primarily upon the acidic properties of CO_2 to cause a subsequently detected change in the pH. In principle, the few pH indicators that have been used to sense CO_2 are subject to many interferences; additionally, the requisite buffers and reference fluorophores add a level of unwanted complexity to the sensing scheme that could be eliminated via the direct detection of CO_2. Efforts to develop a direct method of optical detection for CO_2 have made use of amines appended to organic fluorophores.[9] Fluorophores such as substituted pyrenes exhibit an observable increase in fluorescence due to a decrease in the photoinduced electron-transfer (PET) quenching as a result of the reaction between the amino functionality and CO_2, forming a carbamic acid or carbamate. The amine/CO_2/carbamate equilibrium can be reversed by the removal of dissolved CO_2 by purging solutions with an inert gas.

In practice, the effects of CO_2 exposure to organic fluorophores containing pendant alkylamines are complicated and solvent-dependent. Previous work has shown that highly basic dipolar aprotic solvents such as dimethyl sulfoxide (DMSO), *N*,*N*-dimethylformamide (DMF), and pyridine (Py) are required for complete conversion of arylalkylamines to their corresponding carbamic acids.[9c] Less basic solvents react with a different stoichiometry to give unwanted ammonium carbamate salts. Decreased PET quenching has also been observed in organic and transition-metal luminophores with appended amines upon protonation.[10] The dual reactivity of the amino functionality complicates the interpretation of the sensing mechanism because changes in the luminescence profile initiated by protonation or N-carboxylation would be indistinguishable from one another, and in the case of the ammonium carbamate ion pair, both outcomes would be observed.

Application of a sensing motif that allows for differentiation between N-carboxylation and protonation is desired. In principle, producing a spectral shift should allow this complication to be deconvoluted from the overall optical response. A spectral shift may be achieved through alteration of the coordination sphere of a transition-metal luminophore

Received: June 14, 2011
Published: November 17, 2011

upon exposure to an analyte. Utilizing simple amines both as ligands and sites for CO_2 binding presents the opportunity for stabilization of the N-carboxylated species and a spectral shift through ligation. The simple amine hydrazine and its *N*-carboxylate, carbazate ($H_2NNHCOO^-$), have been known for quite some time to undergo complexation with a large variety of transition-metal ions.[11] The study of this well-defined carbamate formation to detect CO_2 by a luminescent shift is the primary focus of this effort.

We report herein the synthesis, characterization, and photophysical properties of the cationic $[Ir(ppy)_2(N_2H_4)_2]X$ [ppy = 2-phenylpyridine, $X^- = CF_3SO_3^-$, OTf^- (**2a**), Cl^- (**2b**)] and neutral $Ir(ppy)_2(H_2NNHCOO)$ (**3**) iridium(III) bis(cyclometalates). The bis(hydrazino) species can be obtained from the parent μ-chloro-bridged dimer using conventional silver reagents for Cl^- abstraction (**2a**) or through direct replacement in the presence of a slight excess of N_2H_4 (**2b**), yielding a synthetically useful silver-free Cl^- abstraction. Exposure of the ligated hydrazine to CO_2 results in a previously unreported luminescent optical response for CO_2. The presence of CO_2 is detected by a red shift in the observed luminescence λ_{max} accompanied by a change in the peak shape. Crystallographic and ^1H NMR data have confirmed the mechanism of response to involve transformation of a neutral monodentate hydrazino ligand to an anionic bidentate carbazate ligand when exposed to CO_2 in solution.

EXPERIMENTAL DETAILS

General Considerations. NMR spectra were recorded on a Varian Unity or Varian Inova 300 MHz instrument. High-resolution electrospray ionization mass spectrometry (HRESIMS) was performed on a Bruker BioTOF II mass spectrometer. All spectra were recorded in commercially available solvents (Sigma-Aldrich, Fischer, and Mallinckrodt Chemicals) and were used as received. The gases CO_2 (99.98% from Minneapolis Oxygen) and N_2 (high-purity grade from Airgas), used as received, were introduced to the samples in a septum closed cell with a needle. The cyclometalated iridium(III) μ-chloro-bridged dimer $[Ir(ppy)_2Cl]_2$ was prepared using the method of Watts from $IrCl_3 \cdot 3H_2O$ (Johnson Matthey) in a refluxing mixture of 3:1 2-methoxyethanol and H_2O.[12] The acetonitrile (ACN) solvento complex $[Ir(ppy)_2(NCCH_3)_2]OTf$ (**1**) was prepared as previously described from $[Ir(ppy)_2Cl]_2$ in ACN using AgOTf in place of $AgPF_6$.[13]

*[Ir(ppy)$_2$(N$_2$H$_4$)$_2$]OTf (**2a**).* **1** (0.100 g, 0.1367 mmol) was dissolved in 5 mL of methanol (MeOH). Excess hydrazine monohydrate (99%; $N_2H_4 \cdot H_2O$, 25 μL) was added to the solution, yielding a green-brown murky reaction mixture. The solution was allowed to stir for 30 min at room temperature and upon settling gave a black precipitate. The solution was run through a Celite pad, giving a clear, bright-yellow solution. The solvent was removed via rotary evaporation, giving the product **2a** as a glassy yellow powder (0.0922 g, 95%). X-ray-quality crystals were grown from the slow evaporation of a CH_2Cl_2/heptane solution. ^1H NMR (300 MHz, DMSO-d_6): δ 9.20 (d, 2H, J = 5.1 Hz), 8.19 (d, 2H, J = 7.5 Hz), 8.01 (t, 2H, J = 7.5 Hz), 7.73 (d, 2H, J = 6.9 Hz), 7.48 (t, 2H, J = 7.2 Hz), 6.83 (t, 2H, J = 6.9 Hz), 6.68 (t, 2H, J = 7.5 Hz), 6.06 (d, 2H, J = 7.5 Hz), 5.77 (d br, 2H, J = 10.5 Hz), 5.61 (d br, 2H, J = 10.5 Hz). HRESIMS (M^+). Calcd for $C_{22}H_{24}IrN_6$: m/z 565.1686. Found: m/z 565.1687.

*[Ir(ppy)$_2$(N$_2$H$_4$)$_2$]Cl (**2b**).* $[Ir(ppy)_2Cl]_2$ (0.0700 g, 0.0653 mmol) was dissolved in a 2:1 mixture of CH_2Cl_2/MeOH and placed under an argon atmosphere. Once the solid had dissolved, hydrazine monohydrate (99%; $N_2H_4 \cdot H_2O$, 25 μL, 0.515 mmol) was added to the reaction mixture and allowed to stir at room temperature for 3 h. The solvent was removed via rotary evaporation, giving the product as a yellow residue. The residue was redissolved in MeOH and precipitated from solution upon the addition of diethyl ether. The resulting yellow solid was filtered on a fritted glass funnel and dried in vacuo to give 0.0726 g of **2b** (93%). ^1H NMR (300 MHz, DMSO-d_6): δ 9.23 (d, 2H, J = 6.0 and 1.2 Hz), 8.19 (d, 2H, J = 7.8 Hz), 8.01 (ddd, 2H, J = 7.6, 7.6, and 1.2 Hz), 7.73 (dd, 2H, J = 7.8 and 1.2 Hz), 7.47 (ddd, 2H, J = 7.2, 5.7, and 1.2 Hz), 6.82 (ddd, 2H, J = 7.6, 7.6, and 1.2 Hz), 6.68 (ddd, 2H, J = 7.6, 7.6, and 1.2 Hz), 6.06 (dd, 2H, J = 7.6 and 1.2 Hz), 5.86 (d br, 2H, J = 10.5 Hz), 5.64 (d br, 2H, J = 10.5 Hz). HRESIMS (M^+). Calcd for $C_{22}H_{24}IrN_6$: m/z 565.1686. Found: m/z 565.1698. Resonances for the distal N−H protons were not observed in DMSO-d_6 for either OTf^- (**2a**) or Cl^- (**2b**) because of rapid exchange with residual H_2O. See the Supporting Information for details.

*Ir(ppy)$_2$(H$_2$NNHCOO) (**3**).* The neutral carbazate species **3** was obtained by two methods, which are described below as method **3a** and method **3b**.

*Method **3a**.* A fresh solution of compound **2a** (0.0250 g, 0.0342 mmol) in MeOH was prepared as described above. The solution was concentrated to ~1 mL and bubbled with CO_2(g) for 30 min at room temperature, resulting in a yellow microcrystalline precipitate. The yellow solid was collected on a fritted glass filter, removing excess MeOH solution. The solid was dried in vacuo to give 0.0182 g of pure compound **3** (92%). For characterization, see below.

*Method **3b**.* The direct synthesis of **3** starting from the μ-chloro-bridged dimer $[Ir(ppy)_2Cl]_2$ was accomplished by redissolving the residue obtained from the synthesis of **2b** in MeOH. The MeOH solution of **2b** was then bubbled with CO_2(g) generated from dry ice for 30 min at room temperature to give a yellow precipitate. The yellow solid was collected on a fritted glass funnel, removing excess MeOH solution, and washed with H_2O and diethyl ether. The solid was dried in vacuo to give 0.0677 g of pure compound **3** (90%). X-ray-quality crystals were grown from the slow evaporation of an acetone/ACN solution. ^1H NMR (300 MHz, DMSO-d_6): δ 9.04 (d, 1H, J = 5.1 Hz), 8.71 (dd, 1H, J = 5.7 and 0.9 Hz), 8.14 (d, 2H, J = 8.1 Hz), 7.95 (t, 2H, J = 7.5 Hz), 7.68 (t, 2H, J = 6.6 Hz), 7.47 (ddd, 1H, J = 6.9, 5.7, and 1.2 Hz), 7.40 (ddd, 1H, J = 7.2, 5.7, and 1.5 Hz), 7.22 (s br, 1H), 6.94 (d br, 1H, J = 8.7 Hz), 6.76 (ddd, 1H, J = 8.7, 7.5, and 1.2 Hz), 6.73 (ddd, 1H, J = 9.0, 7.8, and 1.5 Hz), 6.60 (ddd, 1H, J = 7.5, 6.6, and 1.5 Hz), 6.57 (ddd, 1H, J = 7.2, 6.0, and 1.2 Hz), 6.41 (d br, 1H, J = 8.7 Hz), 6.20 (dd, 1H, J = 7.8 and 1.2 Hz), 5.94 (dd, 1H, J = 7.8 and 1.2 Hz). HRESIMS (M + Na^+). Calcd for $C_{23}H_{19}IrN_4NaO_2$: m/z 599.1029. Found: m/z 599.1045.

X-ray Structural Determination. The data for the structural determination were collected in the X-ray Crystallographic Lab in the LeClair-Dow Instrumentation Facility (Department of Chemistry, University of Minnesota). Single crystals of compounds **2a** and **3** were placed on a glass capillary and mounted on a Bruker SMART platform CCD diffractometer for **2a** and on a Siemens SMART platform CCD diffractometer for **3** for data collection at 173(2) K using a graphite monochromator and Mo Kα radiation (λ = 0.710 73 Å). An initial set of cell constants was calculated from reflections harvested from three sets of 20 frames such that orthogonal wedges of reciprocal space were surveyed. Final cell constants were determined from a minimum of 2595 strong reflections from the actual data collection. Data were collected to the extent of 1.5 hemispheres to a resolution of 0.77 Å for **2a** and 0.84 Å for **3**. Four major sections of frames were collected with 0.30° steps in ω. The intensity data were corrected for absorption and decay using *SADABS*.[14] The space groups $P2_1/c$ (**2a**) and $P\bar{1}$ (**3**) were determined based on systematic absences and intensity statistics. Direct-method solutions provided the positions of most non-hydrogen atoms. Full-matrix least-squares/difference Fourier cycles were performed to locate the remaining non-hydrogen atoms. All non-hydrogen atoms were refined with anisotropic displacement parameters, and all hydrogen atoms were placed in ideal positions and refined as riding atoms with relative isotropic displacement parameters. All calculations were performed using the *SHELXTL* suite of programs.[15] Further discussion of the cyclometalating ppy ligand ring assignment and a detailed comparison of the N−N hydrazino bond lengths can be found in the Supporting Information.

Optical Spectroscopy and Luminescence Lifetimes. Absorption spectra of the iridium(III) bis(cyclometalates) were collected in a DMSO solution using a 1-cm-path-length quartz cell with a Cary 14

Scheme 1. Synthesis of Iridium(III) Hydrazino and Carbazate Complexes

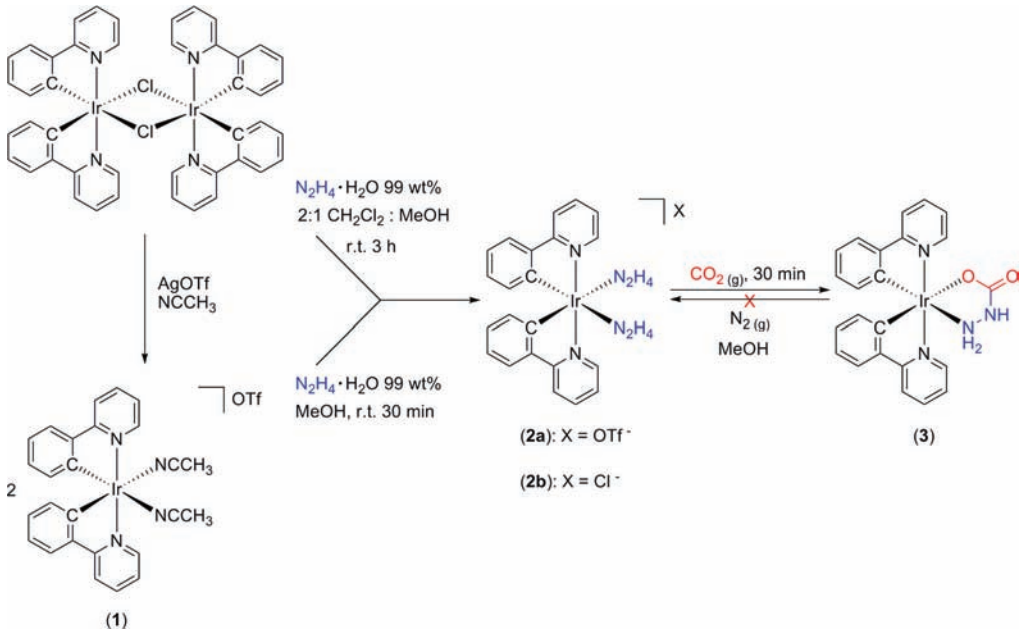

spectrophotometer running the *OLIS globalworks* software suite. Photoluminescence experiments used to obtain luminescence quantum yields were obtained with an excitation wavelength of 400 nm in DMSO using a front-face geometry, with optical densities of solutions >2.0. Data were collected on a Spex Fluorolog 1680 0.2 m double spectrofluorimeter, equipped with a Hamamatsu R928 photomultiplier tube (PMT), running *Datamax* software. Solutions of the iridium(III) bis(cyclometalates) were deaerated ≥60 min prior to collection using an argon purge. All spectra were corrected for the wavelength dependence of the detector. Luminescence quantum yields (ϕ_{em})[16] were measured relative to *fac*-Ir(ppy)$_3$ in deaerated toluene (ϕ_{em} = 0.40), and estimated absolute uncertainties in ϕ_{em} measurements are ±20%; the precision is much better. The luminescence spectra used to monitor the CO_2 gas exposure experiments were obtained using a light-emitting diode (LED) as the source of excitation (λ_{ex} = 405 nm) and a bifurcated fiber optic with front-face detection. Data were collected using an Ocean Optics Inc. charge-coupled-device (CCD) spectrophotometer connected to a computer running the *OOIBase32* software suite (version 2.0.6.5). In this case, the spectra displayed were not corrected for detector response.

Luminescence lifetimes were obtained in solution with an in-house-constructed circuit that pulses a 405 nm LED for excitation of the sample. The light was conducted through one leg of a bifurcated fiber-optic probe to a cuvette that contained a DMSO solution of either **2a** or **3**. The cuvette was deaerated by sparging the solution with N_2. The luminescence decay and scattered light were collected by the other fiber-optic leg, filtered through a cut-off filter to remove the scattered excitation light, and conducted to a Hamamatzu R928 PMT. The PMT signal was digitized by a sampling digital oscilloscope (Phillips PM 3323) interfaced to a computer running a *LabView* program. More details concerning the lifetime data acquisition and processing were previously presented.[17]

RESULTS AND DISCUSSION

Synthesis. The iridium(III) hydrazino complexes [Ir(ppy)$_2$(N_2H_4)$_2$]X [X = OTf^- (**2a**), Cl^- (**2b**)] were synthesized in near-quantitative yield from either the bis(acetonitrile) solvento complex (**1**)[13] or directly from the parent μ-chloro-bridged dimer [Ir(ppy)$_2$Cl]$_2$ at room temperature[12] (Scheme 1). The direct substitution of ligated Cl^- for a neutral monodentate ligand is unique to the N_2H_4 molecule and is attributed to its electron-rich character. Previous examples of direct Cl^- substitution have only been observed in the preparation of anionic [Ir(C^N)(L)$_2$]$^-$ (C^N = cyclometalating ligand) species where L = CN^-, NCS^-, or NCO^-.[18] Attempts to directly obtain analogous cationic [Ir(ppy)$_2$(L$_2$)]$^+$ species where L = alkyl primary amine (*i*-PrNH$_2$) or imine (Py) were unsuccessful; our results and work by Chin et al. indicate that the use of silver reagents would be required for efficient chloride abstraction.[19] Compounds **2a** and **2b** display nearly identical ^{1}H NMR spectra. The introduction of two hydrazino ligands into the coordination sphere of the metal was confirmed by ^{1}H NMR as evidenced by the observation of two broad doublets at 5.61 and 5.77 ppm corresponding to the pair of diastereotopic protons located on the iridium(III)-ligated nitrogen atoms of the hydrazino moiety (Figure 1a, species

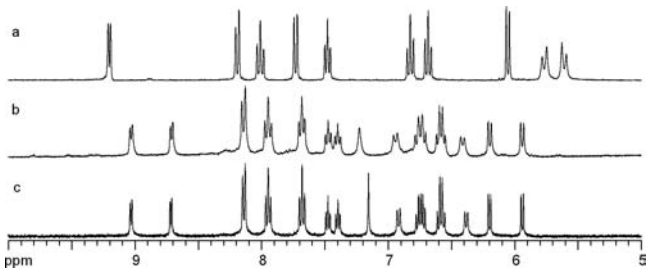

Figure 1. ^{1}H NMR (DMSO-d_6) of (a) **2a**, (b) **3** in situ, and (c) **3** synthetic.

2a only).[20] This assignment was further supported by the presence of eight ppy ligand ^{1}H signals present from 6.0 to 9.5 ppm indicative of a C_2-symmetry coordination sphere.

Complete conversion of the hydrazino complex **2a** to the carbazate complex **3** takes place by the reaction of **2a** with CO_2 in solution. The result of bubbling CO_2 through a sample of **2a** in DMSO-d_6 for 60 min gives the in situ conversion of **2a** to **3** and the ^{1}H NMR spectrum shown in Figure 1b. A comparison of the ^{1}H NMR spectra for **2a** and **3** reveals an increase in the number of ^{1}H signals from 10 to 14, as expected upon conversion from a symmetric (~C_2) to an asymmetric

dx.doi.org/10.1021/ic201286k | *Inorg. Chem.* 2011, 50, 12477–12485

coordination sphere (Figure 1). The most telling peak in the spectrum of **3** is the appearance of a broad singlet between 7.15 and 7.23 ppm corresponding to the presence of an amide, indicating that N-carboxylation of the ligated hydrazine has occurred. Chelation of the *N*-carboxylate moiety results in the loss of the second hydrazino ligand,[21] leading to the formation of a bidentate carbazate ligand. The newly formed **3** is a neutral iridium(III) trischelate, as opposed to its monocationic parent **2a**. Attempts to reverse the reaction of **2a** with CO_2 by bubbling the newly formed solution of **3** with N_2 gave no reaction. Compound **3** was also isolated on a preparative scale from the two different pathways outlined in Scheme 1. The first involves bubbling CO_2 through a concentrated solution of **2a** in MeOH to afford **3** as a yellow microcrystalline precipitate. The second generates **3** directly from the μ-chloro-bridged dimer $[Ir(ppy)_2Cl]_2$ after exposure to a slight excess of hydrazine at room temperature to generate the intermediate **2b** followed by exposure to CO_2. A comparison of the ^{1}H NMR spectra in DMSO-d_6 of the products obtained by both methods to the spectrum of the species generated in situ revealed them to be **3** in each case (Figure 1).

X-ray Crystallography. Single crystals of X-ray quality were grown for compounds **2a** and **3** by slow evaporation from mixtures of CH_2Cl_2/heptane and acetone/ACN, respectively. Relevant crystallographic information for **2a** and **3** is shown in Table 1, and a list of selected bond lengths and angles can be found in Table 2. Compounds **2a** and **3** are the first biscyclometalated iridium(III) species containing a monodentate hydrazine and an unsubstituted carbazate ligand, respectively, to be characterized crystallographically. The structures obtained for compounds **2a** and **3** display two ppy ligands in the *mer* or C,C-*cis*/N,N-*trans* arrangement about a pseudooctahedral iridium(III) center (Figure 2). A set of monodentate N_2H_4 ligands (**2a**) and a bidentate anionic N,O-bound $H_2NNHCOO^-$ (**3**) occupy the remaining two coordination sites in the structures, with both ancillary ligand sets trans to the metalated ppy carbon atoms. The hydrazino N−N bond lengths for **2a** are 1.461(7) and 1.454(8) Å for atoms N3−N4 and N5−N6, respectively, in good agreement with the free hydrazine N−N bond length (1.45 Å).[22] In the case of **3**, the N−N bond length found for atoms N3 and N4 is 1.424(6) Å.

Electronic Spectroscopy. The absorption and luminescence spectra collected for the iridium(III) hydrazino (**2a**) and carbazate (**3**) species are shown in Figure 3. The corresponding spectral data are summarized in Table 3. Both **2a** and **3** display an intense high-energy band at ca. 265 nm (not displayed in Figure 3) and a series of moderate-to-weak absorption shoulders from ca. 340 to 500 nm, as expected for biscyclometalated iridium(III) species.[18,23] The high-energy transitions have been typically assigned as the allowed $^1\pi \rightarrow \pi^*$ transitions centered on the cyclometalating ppy ligands. The remaining moderately intense absorption shoulders and weak absorption tails are labeled as either singlet metal-to-ligand charge-transfer (^{1}MLCT) or triplet metal-to-ligand charge-transfer (^{3}MLCT) transitions ($d\pi_{Ir^{III}} \rightarrow \pi^*_{C\wedge N}$) because of the absence (hydrazino) or noninvolvement (carbazate) of the ancillary ligand (L = neutral monodentate or L^X = anionic bidentate) π-system with frontier orbitals. The electronic differences imparted on the iridium(III) center by the ancillary hydrazino (L) and carbazate (L^X) ligands in the cationic **2a** and neutral **3** result in a 26 nm (1310 cm^{-1}) shift in the lowest-energy ^{1}MLCT transition from 432 (**2a**) to 458 (**3**) nm.

Table 1. Crystallographic Data and Refinement Parameters for the Iridium(III) Hydrazino (2a) and Carbazate (3) Complexes

	$[Ir(ppy)_2(N_2H_4)_2]$ OTf (**2a**)	$Ir(ppy)_2(H_2NNHCOO)$ (**3**)
empirical formula	$C_{23}H_{26}F_3IrN_6O_4S$	$C_{25}H_{26}IrN_5O_4$
cryst color, morphology	yellow, needle	yellow, plate
cryst syst	monoclinic	triclinic
space group	$P2_1/c$	$P\bar{1}$
a, Å	15.024(3)	8.7740(6)
b, Å	9.7170(19)	9.4310(7)
c, Å	18.813(4)	16.2130(12)
α, deg	90	98.9020(10)
β, deg	109.883(3)	92.7260(10)
γ, deg	90	109.0090(10)
volume (V), Å^3	2582.8(9)	1246.24(16)
Z	4	2
fw, g mol^{-1}	731.76	652.71
density (calcd), g cm^{-3}	1.882	1.739
temperature, K	173(2)	173(2)
abs coeff (μ), mm^{-1}	5.314	5.397
F(000)	1432	640
θ range, deg	1.44−27.57	1.44−27.57
index ranges	$-18 \le h \le 19$	$-10 \le h \le 10$
	$-12 \le k \le 12$	$-11 \le k \le 11$
	$-24 \le l \le 24$	$-19 \le l \le 19$
reflns collected	26 779	12 462
indep reflns	5858 [R_{int} = 0.0652]	4412 [R_{int} = 0.0375]
weighting factors,[a] a, b	0.0688, 2.8073	0.0283, 1.3791
max, min transmn	0.7770, 0.1764	0.8905, 0.3831
data/restraints/ parameters	5858/0/343	4412/3/316
R1, wR2 [$I > 2\sigma(I)$]	0.0412, 0.1011	0.0270, 0.0617
R1, wR2 (all data)	0.0683, 0.1164	0.0354, 0.0656
GOF	1.068	1.091
largest diff peak, hole, e Å^{-3}	3.137, −3.129	1.191, −0.956

[a] $w = [\sigma^2(F_o^2) + (aP)^2 + (bP)]^{-1}$, where $P = (F_o^2 + 2F_c^2)/3$.

Table 2. Selected Bond Lengths and Angles for Iridium(III) Hydrazino (2a) and Carbazate (3) Complexes

compound	atoms	bond length (Å)	atoms	bond angle (deg)
2a	Ir1−N1	2.039(5)	N1−Ir1−C1	81.0(2)
	Ir1−N2	2.033(5)	N2−Ir1−C12	79.9(3)
	Ir1−C1	2.032(6)	N3−Ir1−N5	85.1(2)
	Ir1−C12	2.004(6)	Ir1−N3−N4	118.4(4)
	Ir1−N3	2.213 (5)	Ir1−N3−N4	119.7(4)
	Ir1−N5	2.192(6)		
	N3−N4	1.461(7)		
	N5−N6	1.454(8)		
3	Ir1−N1	2.025(4)	N1−Ir1−C11	80.45(19)
	Ir1−N2	2.037(4)	N2−Ir1−C22	80.04(18)
	Ir1−C11	1.985(5)	N3−Ir1−O2	76.96(14)
	Ir1−C22	2.004(5)	Ir1−N3−N4	108.5(3)
	Ir1−N3	2.176(4)		
	Ir1−O2	2.173(3)		
	N3−N4	1.424(6)		
	N4−C23	1.339(7)		
	O1−C23	1.261(6)		
	O2−C23	1.297(6)		

dx.doi.org/10.1021/ic201286k | *Inorg. Chem.* 2011, 50, 12477−12485

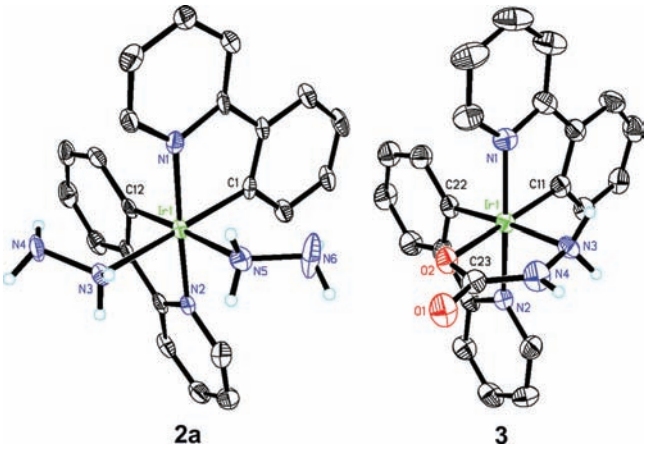

Figure 2. Thermal ellipsoid plots representing 50% probability of **2a** and **3**, with ppy hydrogen atoms, molecules of solvation, and the OTf^- counterion (**2a**) omitted for clarity.

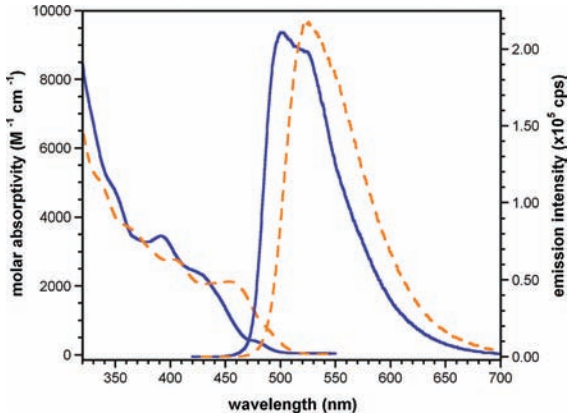

Figure 3. Absorption and luminescence spectra of **2a** (blue —) and **3** (orange - - -) in deaerated DMSO at 298 K (λ_{ex} = 400 nm).

Table 3. Photophysical Properties[a] of Iridium(III) Hydrazino (2a) and Carbazate (3) Complexes

compound	λ_{abs}, nm (ε, $\times 10^4$ M^{-1} cm^{-1})	λ_{em},[b] nm	ϕ_{em}[c,d]	τ_{em},[e] μs
2a	264 (3.13), 350 (0.49), 393 (0.34), 432 (0.22), 480 (0.03)	501	0.42	1.56(1)
3	267 (2.63), 338 (0.49), 365 (0.36), 408 (0.27), 458 (0.21), 490 (0.07)	524	0.45	1.80(1)

[a]All spectra recorded in deaerated DMSO solutions at 298 K. [b]λ_{ex} = 400 nm. [c]Determined relative to *fac*-Ir(ppy)$_3$ in toluene (ϕ_{em} = 0.40).[16] [d]Considered accurate to ±20%. [e]λ_{ex} = 405 nm.

The iridium(III) hydrazino (**2a**) and carbazate (**3**) species both display strong luminescence in deaerated DMSO solutions at room temperature (Figure 3) and were found to have similar phosphorescence lifetimes (τ = 1.56 and 1.80 μs, respectively) and luminescence quantum yields (ϕ_{em} = 0.42 and 0.45, respectively). As observed for the absorption spectra, a 23 nm (876 cm^{-1}) red shift in the luminescence λ_{max} between **2a** and **3** highlights the differences in the electronic structure at the iridium(III) center. Also apparent is the loss of band structure in the luminescence profile of the carbazate species **3**. Of particular interest are the photophysical properties of the iridium(III) cabazate species **3**, which represents a new addition to the family of luminescent iridium(III) bis(cyclometalates) of the type Ir(C^N)$_2$(L^X). Phosphorescence lifetime and quantum yield measurements are similar to those of the related Ir(ppy)$_2$(acac) (acac = acetylacetonate) species (τ = 1.6 μs and ϕ_{em} = 0.34)[23d] and indicate the potential use of **3** as a triplet sensitizer or phosphorescent dopant in electroluminescent devices.

Optical Response to CO_2. The successful conversion of amine bearing fluorophores to carbamic acids by exposure to CO_2 has been shown to be highly solvent-dependent.[9a,c] Solvents found suitable by previous investigators are DMSO, DMF, and Py, while ACN, $CHCl_3$, 2-propanol, CH_3OH, benzene, dioxane, and tetrahydrofuran were named as unsuitable. The luminescence of **2a** was monitored in DMSO, DMF, CH_3OH, ACN, and $CHCl_3$ solutions under steady streams of both N_2 and CO_2 gas. No change was observed for solutions of **2a** under N_2 gas, with the exception of $CHCl_3$, where the solution darkened over time, leading to decomposition. Exposure of the remaining solutions to CO_2 showed a red shift in the luminescence λ_{max} of **2a** upon conversion to the luminescent carbazate species **3** (Figure 4). Completion times for conversion of **2a** to **3** were solvent-dependent, with the fastest in DMSO and DMF and the slowest in MeOH and ACN.

As far as we know, optical responses from motifs employing the amine/carbamate equilibrium to CO_2 have been limited to intensity changes. A novel optical sensing scheme using carbonate (from CO_2) to modulate the luminescence of a solvatochromic probe by altering the probe's local environment has been reported.[8a] The sensing response, based on changes in the polarity rather than the pH, is formally a method of indirect detection. The observation of a spectral shift in the luminescence λ_{max} as the optical response within the amine/carbamate motif has not yet been reported. The optical response of the iridium(III) hydrazine system described here is due to the direct involvement of the amine/carbamate conversion with the coordination sphere of the transition-metal chromophore. The conversion of **2a** to **3** results in changes to the iridium(III) coordination sphere shifting the relative energies of the lowest-lying excited states. These shifts likely contribute significant ^{3}MLCT character to the lowest-energy excited state, which is a mixture of triplet ligand-centered (^{3}LC)/^{3}MLCT states and results in the loss of the vibrational structure observed in the luminescence profile.[24]

Two competitive pathways to N-carboxylation have been outlined for amine/carbamate systems.[9] The first results from an initial reaction of the amine with CO_2, followed by proton transfer to a second amine to form an ammonium carbamate ion pair [RR′NCOO$^-$] [RR′NH$_2^+$]. The second involves direct protonation of the amine via formation of carbonic acid, in situ forming an ammonium bicarbonate ion pair [HCO_3^-]-[RR′NH$_2^+$]. In an effort to understand which of the two previously observed pathways may be operative in the iridium(III) hydrazine system described here, 2 equiv of trifluoroacetic acid (TFA) was added to a NMR tube of **2a** in DMSO-d_6. A deaerated sample of **2a** in DMSO-d_6 is intensely luminescent and gives the ^{1}H NMR spectrum shown in Figure 5a. It was found that the addition of acid resulted in a dramatic decrease of the luminescence of the sample and the ^{1}H NMR spectrum shown in Figure 5b. The loss of both hydrazino ligands is evidenced by the absence of Ir−NH$_2$ ^{1}H signals at 5.61 and 5.77 ppm (Figure 5b).

These results suggest that protonation of the hydrazino ligands, to give coordinated $H_2NNH_3^+$, sufficiently weakens the

dx.doi.org/10.1021/ic201286k | Inorg. Chem. 2011, 50, 12477−12485

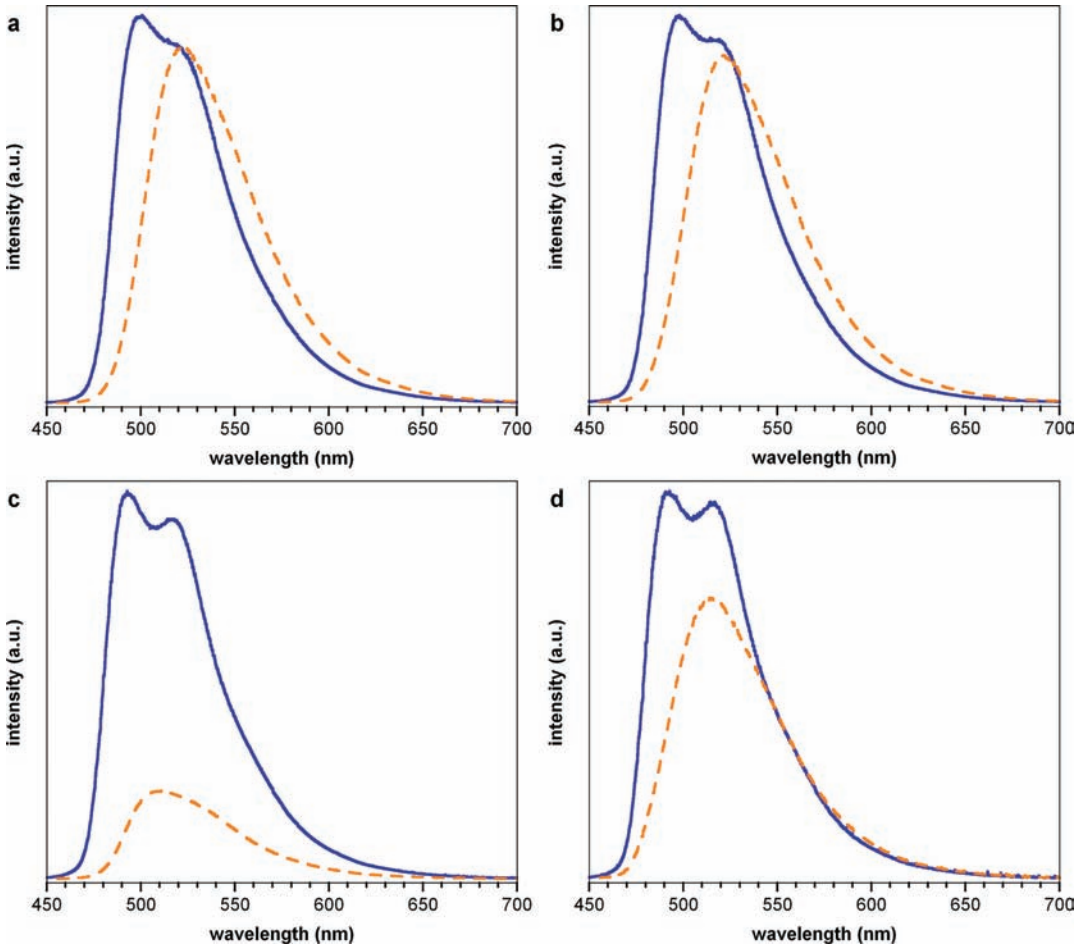

Figure 4. Uncorrected luminescence spectra at 298 K (λ_{ex} = 405 nm) of **2a** before (blue —) and after (orange - - -) exposure to CO_2 in (a) DMSO (60 min), (b) DMF (50 min), (c) MeOH (7 h), and (d) ACN (14 h). For each solvent, the spectra are normalized to the initial intensity of **2a** prior to CO_2 exposure.

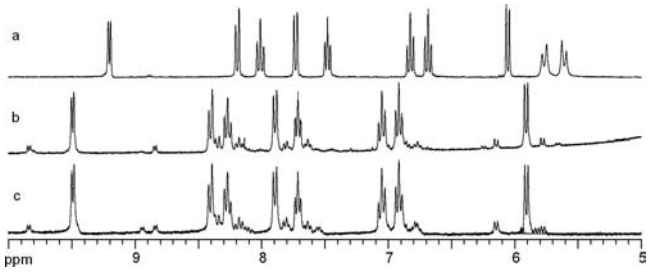

Figure 5. ^{1}H NMR DMSO-d_6 of (a) **2a**, (b) $[Ir(ppy)_2(DMSO)_2]^+$ after the addition of TFA to **2a**, and (c) $[Ir(ppy)_2(DMSO)_2]^+$ prepared by dissolving **1** in DMSO-d_6.

Ir−N bond to cause subsequent displacement of $H_2NNH_3^+$ by the surrounding solvent to form the DMSO bis-solvento complex $[Ir(ppy)_2(DMSO)_2]^+$ (**4**; Scheme 2b). The identity of this species was confirmed as **4** after a comparison of the ^{1}H NMR spectrum seen in parts b and c of Figure 5 containing **4** generated by the addition of **1** to DMSO-d_6. The extremely weak luminescence of **4** has also been observed for similar solvento complexes including **1** and further supports this assignment.[13b]

Because conversion of **2a** to **3** during CO_2 exposure experiments does not yield the immediate and near total loss of luminescence observed for protonation, we propose that the primary event that occurs during CO_2 exposure is N-carboxylation and not protonation (Scheme 2). This result also eliminates the uncertainty of quenching originating from protonation or N-carboxylation. The formation of an ammonium carbonate ion pair followed by the loss of $H_2NNH_3^+$ in sequence for both hydrazino ligands is expected to provide a result similar to that observed for the addition of TFA, namely, the formation of the bis-solvento complex rather than the carbazate complex **3**.

Elimination of the direct protonation pathway suggests that formation of an ammonium carbamate ion-pair intermediate (Scheme 2a) is the more likely scenario. The iridium(III) hydrazine system here contains two potential CO_2 binding sites, one for each of the hydrazino ligands. After N-carboxylation of one hydrazino ligand occurs, proton transfer to the second is possible, leading to the formation of a "backside" metal-coordinated ammonium carbamate ion pair $[MH_2NNHCOO^-][MH_2NNH_2^+]$. This outcome should lead to the loss of a single hydrazino ligand as $H_2NNH_3^+$, followed by immediate chelation of the bidentate carbazate moiety to form the neutral iridium(III) carbazate species **3**.

Several preliminary kinetic runs using luminescence spectroscopy to follow the conversion of the bis(hydrazino) species to the resulting carbazate were made to further investigate the optical response observed upon exposure of **2a** to CO_2. Data were obtained by collecting full-frequency steady-state emission spectra versus time during exposure of **2a** to CO_2 in DMSO

Scheme 2. Competitive Pathways to N-Carboxylation in the Iridium(III) Hydrazine System: (a) N-Carboxylation followed by Proton Transfer and (b) Direct Protonation

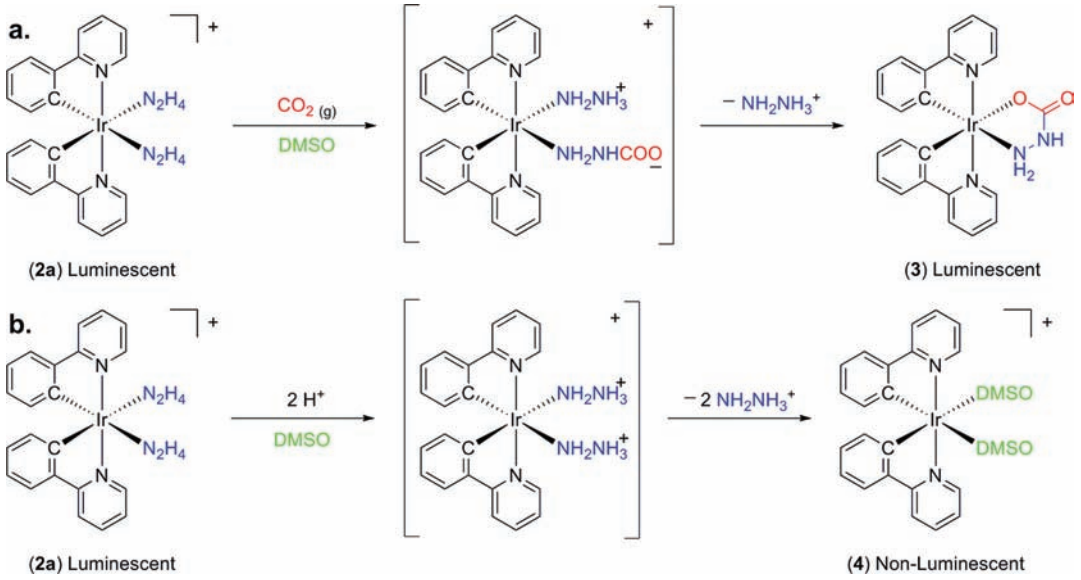

solutions at room temperature. From these data, three wavelengths (500, 522, and 550 nm) that exhibited significant variation in the observed emission intensity during CO_2 exposure were selected. The intensity versus time data for these three wavelengths were simultaneously fit to an irreversible, consecutive first-order reaction kinetic scheme. Three independent runs resulted in similar response functions and gave k_1 = 0.02(1) s^{-1} and k_2 = 0.0015(3) s^{-1}, which indicated variation in the values for the rapid first process (k_1), while the values for the second process (k_2) were more consistent [see the Supporting Information for an example kinetic plot (Figure S4)].

Analysis of these data suggests the fast, irreversible formation of an intermediate species upon exposure of **2a** to CO_2 in DMSO represented by k_1, followed by the comparatively slower irreversible conversion to the carbazate species **3** represented by k_2. These results are consistent with the pathway depicted in Scheme 2a, which involves the initial rapid binding of CO_2 by **2a** to form a mondentate carbazate intermediate and the slower replacement of the second hydrazino ligand to form the final bidentate carbazate species **3**. Results obtained from these preliminary kinetic runs support the primary event as being N-carboxylation, although it is unclear what the exact composition of the intermediate is; the possibility of a doubly N-carboxylated intermediate cannot be ruled out at this time. The second process involves the loss of hydrazine from the coordination sphere and replacement by the N-carboxylated terminus of the remaining monodentate carbazate ligand. It is unclear whether this is a stepwise or concerted process. Although this system shows the desired reactivity, it demonstrates limited utility because of solvent dependence and the lack of reversibility. Collection of the standard analytical chemistry metrics and more detailed kinetic studies that could fully characterize a working sensor scheme will need to await a faster and reversible system.

■ CONCLUSIONS

We have prepared novel hydrazino and carbazate transition-metal species through coupling of a luminescent biscyclometalated iridium(III) core with the well-defined chemistry between hydrazine and CO_2. The incorporation of hydrazine into the synthetic pathway was found to be an attractive and simple means for chloride abstraction. Treatment of the bis-(hydrazino) species with a stoichiometric portion of a proton source has been found to be an alternative means of preparing the labile Cl^--free bis-solvento species. Alternatively, exposure of the bis(hydrazino) species to CO_2, thereby generating the corresponding neutral carbazates, provides a new synthetic strategy for the preparation of a family of neutral luminescent Ir(C^N)$_2$(L^X)-type complexes. This system has been well characterized, and the products of CO_2 exposure have been determined by ^{1}H NMR and X-ray crystallography, demonstrating the utility of ligated N_2H_4 as a site for CO_2 binding.

The attractive photophysical properties of this system were exploited to develop a scheme for the direct optical detection of CO_2 based on hydrazine/carbazate conversion. The excited states of both the hydrazino and carbazate complexes have long lifetimes (~1.5 μs) and high emission quantum yields (~0.4) in room temperature DMSO solutions. The reaction of the hydrazino complex with CO_2 affords the first instance of a spectroscopic shift in emission λ_{max} as the optical response to CO_2 exposure within the amine/carbamate motif. Carbamic acids are known to be unstable, preferring the unprotonated anionic carbamate form, requiring a basic site for proton transfer. The iridium(III) hydrazine system developed here benefits from having two available sites for either N-carboxylation or protonation within the same luminophore. The 2:1 amine/CO_2 stoichiometry separates protonation from N-carboxylation through the loss of the protonated hydrazine while retaining the N-carboxylated moiety. Stabilization of the N-carboxylated hydrazino ligand through coordination provides the unique optical response of a 23 nm red shift in the luminescence λ_{max}. Although the iridium(III) hydrazine system exhibits slow reaction times, unwanted solvent dependence, and irreversible binding of CO_2, this work is a first step toward achieving a reliable method for the direct optical detection of CO_2.

dx.doi.org/10.1021/ic201286k | Inorg. Chem. 2011, 50, 12477–12485

■ ASSOCIATED CONTENT

Supporting Information

Crystallographic data in CIF format for **2a** and **3**, additional structural discussion, ^{1}H NMR spectra of $[Ir(ppy)_2(N_2H_4)_2]$-PF_6 in *o*-dichlorobenzene-d_4, luminescence decay plots for **2a** and **3**, and emission intensity versus time curves at three wavelengths. This material is available free of charge via the Internet at http://pubs.acs.org.

■ AUTHOR INFORMATION

Corresponding Author

*E-mail: krmann@umn.edu.

■ ACKNOWLEDGMENTS

The authors thank the Center for Process Analytical Chemistry at the University of Washington (for the sensing studies) and the Department of Energy (for synthesis of the compounds) for partial support of this research.

■ REFERENCES

(1) (a) Farrer, N. J.; Salassa, L.; Sadler, P. J. *Dalton Trans.* **2009**, 10690. (b) Fukuzumi, S.; Ohkubo, K.; Zheng, X.; Chen, Y.; Pandey, R. K.; Zhan, R.; Kadish, K. M. *J. Phys. Chem. B* **2008**, *112*, 2738. (c) Gianferrara, T.; Bergamo, A.; Bratsos, I.; Milani, B.; Spagnul, C.; Sava, G.; Alessio, E. *J. Med. Chem.* **2010**, *53*, 4678. (d) Lai, C.-W.; Wang, Y.-H.; Lai, C.-H.; Yang, M.-J.; Chen, C.-Y.; Chou, P.-T.; Chan, C.-S.; Chi, Y.; Chen, Y.-C.; Hsiao, J.-K. *Small* **2008**, *4*, 218. (e) Liu, Y.; Hammitt, R.; Lutterman, D. A.; Joyce, L. E.; Thummel, R. P.; Turro, C. *Inorg. Chem.* **2009**, *48*, 375.

(2) (a) Goodrich, L. E.; Paulat, F.; Praneeth, V. K. K.; Lehnert, N. *Inorg. Chem.* **2010**, *49*, 6293. (b) Schopfer, M. P.; Wang, J.; Karlin, K. D. *Inorg. Chem.* **2010**, *49*, 6267. (c) Tonzetich, Z. J.; McQuade, L. E.; Lippard, S. J. *Inorg. Chem.* **2010**, *49*, 6338.

(3) (a) Fontaine, P. P.; Yonke, B. L.; Zavalij, P. Y.; Sita, L. R. *J. Am. Chem. Soc.* **2010**, *132*, 12273. (b) Fryzuk, M. D.; Johnson, S. A. *Coord. Chem. Rev.* **2000**, *200–202*, 379. (c) Gilbertson, J. D.; Szymczak, N. K.; Tyler, D. R. *J. Am. Chem. Soc.* **2005**, *127*, 10184. (d) Laplaza, C. E.; Cummins, C. C. *Science* **1995**, *268*, 861. (e) Lee, Y.; Mankad, N. P.; Peters, J. C. *Nat. Chem.* **2010**, *2*, 558. (f) MacKay, B. A.; Fryzuk, M. D. *Chem. Rev.* **2004**, *104*, 385. (g) Pool, J. A.; Lobkovsky, E.; Chirik, P. J. *Nature* **2004**, *427*, 527. (h) Yandulov, D. V.; Schrock, R. R. *Science* **2003**, *301*, 76.

(4) (a) Blakemore, J. D.; Schley, N. D.; Balcells, D.; Hull, J. F.; Olack, G. W.; Incarvito, C. D.; Eisenstein, O.; Brudvig, G. W.; Crabtree, R. H. *J. Am. Chem. Soc.* **2010**, *132*, 16017. (b) Concepcion, J. J.; Jurss, J. W.; Templeton, J. L.; Meyer, T. J. *J. Am. Chem. Soc.* **2008**, *130*, 16462. (c) Gagliardi, C. J.; Westlake, B. C.; Kent, C. A.; Paul, J. J.; Papanikolas, J. M.; Meyer, T. J. *Coord. Chem. Rev.* **2010**, *254*, 2459. (d) McDaniel, N. D.; Coughlin, F. J.; Tinker, L. L.; Bernhard, S. *J. Am. Chem. Soc.* **2008**, *130*, 210. (e) Wasylenko, D. J.; Ganesamoorthy, C.; Koivisto, B. D.; Henderson, M. A.; Berlinguette, C. P. *Inorg. Chem.* **2010**, *49*, 2202. (f) Yin, Q.; Tan, J. M.; Besson, C.; Geletii, Y. V.; Musaev, D. G.; Kuznetsov, A. E.; Luo, Z.; Hardcastle, K. I.; Hill, C. L. *Science* **2010**, *328*, 342. (g) Zong, R.; Thummel, R. P. *J. Am. Chem. Soc.* **2005**, *127*, 12802.

(5) (a) Federsel, C.; Jackstell, R.; Beller, M. *Angew. Chem., Int. Ed.* **2010**, *49*, 6254. (b) Himeda, Y. *Eur. J. Inorg. Chem.* **2007**, *2007*, 3927. (c) Sadique, A. R.; Brennessel, W. W.; Holland, P. L. *Inorg. Chem.* **2008**, *47*, 784. (d) Silvia, J. S.; Cummins, C. C. *J. Am. Chem. Soc.* **2010**, *132*, 2169. (e) van der Boom, M. E. *Angew. Chem., Int. Ed.* **2009**, *48*, 28.

(6) (a) Chen, B.; Ma, S.; Hurtado, E. J.; Lobkovsky, E. B.; Zhou, H.-C. *Inorg. Chem.* **2007**, *46*, 8490. (b) Demessence, A.; D'Alessandro, D. M.; Foo, M. L.; Long, J. R. *J. Am. Chem. Soc.* **2009**, *131*, 8784. (c) Keskin, S.; van Heest, T. M.; Sholl, D. S. *ChemSusChem* **2010**, *3*, 879. (d) Millward, A. R.; Yaghi, O. M. *J. Am. Chem. Soc.* **2005**, *127*, 17998. (e) Phan, A.; Doonan, C. J.; Uribe-Romo, F. J.; Knobler, C. B.; O'Keeffe, M.; Yaghi, O. M. *Acc. Chem. Res.* **2009**, *43*, 58.

(7) (a) Amao, Y.; Nakamura, N. *Sens. Actuators, B* **2004**, *100*, 347. (b) Amao, Y.; Nakamura, N. *Sens. Actuators, B* **2005**, *107*, 861. (c) Darwish, T. A.; Evans, R. A.; James, M.; Malic, N.; Triani, G.; Hanley, T. L. *J. Am. Chem. Soc.* **2010**, *132*, 10748. (d) DeGrandpre, M. D. *Anal. Chem.* **1993**, *65*, 331. (e) Fernández-Sánchez, J. F.; Cannas, R.; Spichiger, S.; Steiger, R.; Spichiger-Keller, U. E. *Sens. Actuators, B* **2007**, *128*, 145. (f) Mills, A.; Lepre, A.; Wild, L. *Sens. Actuators, B* **1997**, *39*, 419. (g) Mills, A.; Skinner, G. A. *Analyst* **2010**, *135*, 1912. (h) Nakamura, N.; Amao, Y. *Anal. Bioanal. Chem.* **2003**, *376*, 642.

(8) (a) Ali, R.; Lang, T.; Saleh, S. M.; Meier, R. J.; Wolfbeis, O. S. *Anal. Chem.* **2011**, *83*, 2846. (b) Borisov, S. M.; Krause, C.; Arain, S.; Wolfbeis, O. S. *Adv. Mater.* **2006**, *18*, 1511. (c) Burke, C. S.; Markey, A.; Nooney, R. I.; Byrne, P.; McDonagh, C. *Sens. Actuators, B* **2006**, *119*, 288. (d) Cajlakovic, M.; Bizzarri, A.; Ribitsch, V. *Anal. Chim. Acta* **2006**, *573–574*, 57. (e) Ertekin, K.; Alp, S. *Sens. Actuators, B* **2006**, *115*, 672. (f) Liu, Y.; Tang, Y.; Barashkov, N. N.; Irgibaeva, I. S.; Lam, J. W. Y.; Hu, R.; Birimzhanova, D.; Yu, Y.; Tang, B. Z. *J. Am. Chem. Soc.* **2010**, *132*, 13951. (g) Nakamura, N.; Amao, Y. *Sens. Actuators, B* **2003**, *92*, 98. (h) Oter, O.; Ertekin, K.; Topkaya, D.; Alp, S. *Anal. Bioanal. Chem.* **2006**, *386*, 1225. (i) Stich, M. I. J.; Fischer, L. H.; Wolfbeis, O. S. *Chem. Soc. Rev.* **2010**, *39*, 3102.

(9) (a) Hampe, E. M.; Rudkevich, D. M. *Tetrahedron* **2003**, *59*, 9619. (b) Herman, P.; Murtaza, Z.; Lakowicz, J. R. *Anal. Biochem.* **1999**, *272*, 87. (c) Masuda, K.; Ito, Y.; Horiguchi, M.; Fujita, H. *Tetrahedron* **2005**, *61*, 213.

(10) (a) Charbonniere, L. J.; Ziessel, R. F.; Sams, C. A.; Harriman, A. *Inorg. Chem.* **2003**, *42*, 3466. (b) de Silva, A. P.; Gunaratne, H. Q. N.; Gunnlaugsson, T.; Huxley, A. J. M.; McCoy, C. P.; Rademacher, J. T.; Rice, T. E. *Chem. Rev.* **1997**, *97*, 1515. (c) de Silva, A. P.; Gunaratne, H. Q. N.; McCoy, C. P. *Chem. Commun.* **1996**, 2399. (d) de Silva, S. A.; Zavaleta, A.; Baron, D. E.; Allam, O.; Isidor, E. V.; Kashimura, N.; Percarpio, J. M. *Tetrahedron Lett.* **1997**, *38*, 2237. (e) Wong, K. H.; Chan, M. C. W.; Che, C. M. *Chem.—Eur. J.* **1999**, *5*, 2845.

(11) (a) Bottomley, F. *Q. Rev. Chem. Soc.* **1970**, *24*, 617. (b) Dilworth, J. R. *Coord. Chem. Rev.* **1976**, *21*, 29. (c) Heaton, B. T.; Jacob, C.; Page, P. *Coord. Chem. Rev.* **1996**, *154*, 193.

(12) Sprouse, S.; King, K. A.; Spellane, P. J.; Watts, R. J. *J. Am. Chem. Soc.* **1984**, *106*, 6647.

(13) (a) McGee, K. A.; Mann, K. R. *Inorg. Chem.* **2007**, *46*, 7800. (b) Schmid, B.; Garces, F. O.; Watts, R. J. *Inorg. Chem.* **1994**, *33*, 9.

(14) (a) Blessing, R. H. *Acta Crystallogr., Sect. A* **1995**, *51*, 33. (b) Sheldrick, G. *SADABS*, version 2.03; Bruker AXS: Madison, WI, 2002.

(15) *SHELXTL*, version 6.1; Bruker AXS: Madison, WI, 2001.

(16) King, K. A.; Spellane, P. J.; Watts, R. J. *J. Am. Chem. Soc.* **1985**, *107*, 1431.

(17) McGee, K. A.; Veltkamp, D. J.; Marquardt, B. J.; Mann, K. R. *J. Am. Chem. Soc.* **2007**, *129*, 15092.

(18) Nazeeruddin, M. K.; Humphry-Baker, R.; Berner, D.; Rivier, S.; Zuppiroli, L.; Graetzel, M. *J. Am. Chem. Soc.* **2003**, *125*, 8790.

(19) Chin, C. S.; Eum, M.-S.; yi Kim, S.; Kim, C.; Kang, S. K. *Eur. J. Inorg. Chem.* **2007**, *2007*, 372.

(20) The proton resonances for the distal N–H hydrogen atoms were not observed for the hydrazino ligands in complexes **2a** or **2b** in DMSO-d_6. The appropriate resonances can be observed in *o*-dichloroenzene-d_4. See the Supporting Information for details.

(21) The appearance of a new resonance for the released hydrazino ligand is not observed because of rapid exchange with residual H_2O in DMSO-d_6.

(22) Schmidt, E. W. *Hydrazine and Its Derivatives: Preperation, Properties, Applications*; John Wiley & Sons: New York, 1984.

(23) (a) Colombo, M. G.; Brunold, T. C.; Riedener, T.; Guedel, H. U.; Fortsch, M.; Buergi, H.-B. *Inorg. Chem.* **1994**, *33*, 545. (b) Garces, F. O.; King, K. A.; Watts, R. J. *Inorg. Chem.* **1988**, *27*, 3464. (c) Hay, P. J. *J. Phys. Chem. A* **2002**, *106*, 1634. (d) Lamansky, S.; Djurovich, P.; Murphy, D.; Abdel-Razzaq, F.; Kwong, R.; Tsyba, I.; Bortz, M.; Mui, B.; Bau, R.; Thompson, M. E. *Inorg. Chem.* **2001**, *40*, 1704.

(e) Ohsawa, Y.; Sprouse, S.; King, K. A.; DeArmond, M. K.; Hanck, K. W.; Watts, R. J. *J. Phys. Chem.* **1987**, *91*, 1047.
(24) Flamigni, L.; Barbieri, A.; Sabatini, C.; Ventura, B.; Barigelletti, F. *Top. Curr. Chem.* **2007**, *281*, 143.